DOI: 10.6060/ivkkt.20196206.6041

УДК: 544.478.023.57

СИНТЕЗ, СТРУКТУРА И КАТАЛИТИЧЕСКИЕ СВОЙСТВА НАНОСТРУКТУРНЫХ Pd МАТЕРИАЛОВ В КАТАЛИТИЧЕСКОЙ ГИДРОГЕНАЦИИ п-НИТРОАНИЛИНА

В.Ю. Долуда, А.И. Сидоров, Э.М. Сульман, А.Р. Латыпова, Д.В. Филиппов, О.В. Лефедова

Валентин Юрьевич Долуда, Александр Иванович Сидоров, Эсфирь Михайловна Сульман

Кафедра биотехнологии и химии, Тверской государственный технический университет, Наб. А. Никитина 22, Тверь, Российская Федерация, 170023
E-mail: doludav@yandex.ru, sidorov_science@mail.ru, sulman@online.tver.ru

Адель Ришатовна Латыпова, Дмитрий Вячеславович Филиппов, Ольга Валентиновна Лефедова*

Кафедра физической и коллоидной химии, Ивановский государственный химико-технологический университет, Шереметевский просп., 7, Иваново, Российская Федерация, 153000
E-mail: LatAdel@yandex.ru, fillipov@isuct.ru, physchem.606@yandex.ru*

Статья посвящена разработке палладиевых катализаторов на носителях, исследованию их структуры, каталитических свойств и их корреляции с активностью катализаторов в гидрировании п-нитроанилина. Серия палладиевых нанесенных катализаторов была синтезирована с использованием носителей: Al_2O_3, SiO_2 и угля АР-Д для стабилизации частиц Pd с загрузкой активного металла 3, 4, 5 мас. долей (%). Образцы катализаторов были синтезированы с использованием метода осаждения и охарактеризованы сканирующей электронной микроскопией, температурно-программируемым восстановлением, физической сорбцией азота, инфракрасной спектроскопией и испытаны в процессе каталитического гидрирования п-нитроанилина. В работе показан эффективный подход получения функциональных материалов с точки зрения применения катализа. Основными преимуществами такого подхода являются дешевизна и простота внедрения, которые дают возможность получать функциональные материалы прямо на месте применения. Все используемые химикаты широко доступны, и дополнительное оборудование не требуется. Активность образцов катализаторов в процессе гидрирования п-нитроанилина имеет сильную корреляцию со значениями дисперсности нанесенного металла и кислотностью носителя. Образец с 5 мас.% Pd/γ-Al_2O_3 показывает наибольшую активность ~ $4{,}6 \cdot 10^{-5}$ моль (H_2)/с., где носитель катализатора характеризуется высокой кислотностью, а нанесенный металл умеренной дисперсностью. Сравнение данных активности катализатора и содержания пор различных размеров показало определенную корреляцию. После реакции гидрирования 4-нитроанилина изменение размеров пор катализаторов может дать косвенную информацию о предполагаемых физических процессах, происходящих на поверхности катализатора. В целом, по полученным результатам была обнаружена корреляция между структурой, физико-химией катализатора и его активностью в гидрировании п-нитроанилина.

Ключевые слова: катализ, палладий, оксид алюминия, кремнезем, углерод, гидрирование

SYNTHESIS, STRUCTURE AND CATALYTIC PROPERTIES OF Pd NANOSTRUCTURED MATERIALS IN p-NITROANILINE CATALYTIC HYDROGENATION

V.Yu. Doluda, A.I. Sidorov, E.M. Sulman, A.R. Latypova, D.V. Filippov, O.V. Lefedova

Valentin Yu. Doluda, Alexander I. Sidorov, Esther M. Sulman

Department of Biotechnology and Chemistry, Tver State Technical University, Nab. A. Nikitina, 22, Tver, 170023, Russia
E-mail: doludav@yandex.ru, sidorov_science@mail.ru, sulman@online.tver.ru

Adele R. Latypova, Dmitry V. Filippov, Olga V. Lefedova*

Department of Physical and Colloid Chemistry, Ivanovo State University of Chemistry and Technology, Sheremetevsky ave., 7, Ivanovo, 153000, Russia
E-mail: LatAdel@yandex.ru, fillipov@isuct.ru, physchem.606@yandex.ru*

The article is focused on development of palladium supported catalysts, investigation of their structure and catalytic properties and correlations of catalysts activity in hydrogenation of p-nitroaniline. A series of Pd supported catalysts were synthesized using Al_2O_3, SiO_2 and activated carbon for Pd stabilization with active metal loading of 3, 4, 5 wt. %. Catalysts samples were synthesized using modified precipitation method, characterized by scanning electron microscopy, temperature programmed reduction, nitrogen physisorption, infrared spectroscopy and tested in p-nitroaniline catalytic hydrogenation process. The work shows efficient approach of functional materials obtainment in terms of catalysis application. Main advantages of such approach are cheapness and ease of implementation, which give the possibility to obtain functional materials right on the place of application. All chemicals used are of wide availability and no additional equipment is necessary. The Pd based catalysts supported on alumina, silica and activated carbon were tested in p-nitroaniline hydrogenation. Catalysts sample activity in p-nitroaniline hydrogenation process has strong correlation with metal dispersion and support acidity. The sample 5 wt.% Pd/γ-Al_2O_3 show the highest activity $4.6 \cdot 10^{-5}$ mol(H_2)/s characterized by highest acidity and moderate metal dispersion. The comparison of the data of catalyst activity and the content of pores of various sizes showed the certain correlation. After the reaction of hydrogenation of 4-nitroaniline, the change in the pore sizes of the catalysts can provide indirect information about the supposed physical processes occurring on the surface of the catalyst. Strong correlation between catalyst structure and its activity in p-nitroaniline hydrogenation was found.

Key words: catalysis, palladium, alumina, silica, carbon, hydrogenation

Для цитирования:
Долуда В.Ю., Сидоров А.И., Сульман Э.М., Латыпова А.Р., Филиппов Д.В., Лефедова О.В. Синтез, структура и каталитические свойства наноструктурных Pd материалов в каталитической гидрогенации п-нитроанилина. *Изв. вузов. Химия и хим. технология*. 2019. Т. 62. Вып. 6. С. 60–68

For citation:
Doluda V.Yu., Sidorov A.I., Sulman E.M., Latypova A.R., Filippov D.V., Lefedova O.V. Synthesis, structure and catalytic properties of Pd nanostructured materials in p-nitroaniline catalytic hydrogenation. *Izv. Vyssh. Uchebn. Zaved. Khim. Khim. Tekhnol.* 2019. V. 62. N 6. P. 60–68

INTRODUCTION

Development of catalytic active nanostructured materials presents a special interest for application in fine organic synthesis of valuable substances [1-4]. Palladium nanoparticulate materials are widely used as catalysts in hydrogenation reactions due to unique catalytic properties including possibility to provide reaction under mild conditions, compare to nanostructured materials containing other transition state metals (Pt, Ru, Ni, Fe etc.) [5-10]. Palladium nanoparticles are ideal catalytic phase for hydrogenation reactions, as it easily dissociates hydrogen molecules under ambient conditions [11]. Typically Pd nanoparticles applicable for catalytic hydrogenation processes are stabilized by different supports including inorganic supports, mainly alumina, silica, titanium dioxide, zeolites and different polymers, including rigid polymer matrixes, polymer micelles and polymer gels [12-18]. Polymers are superior in stabilization of metal nanoparticles compare to inorganic supports, however, application of such systems for catalytic hydrogenation have several disadvantages, including rapid nanoparticles sintering in organic reaction media under high reaction pressure and temperature [19, 20]. Therefore application of traditionally used inorganic supports can be also attractive for synthesis of stable Pd nanoparticulate systems for application in catalysis [21, 22]. However obtaining high dispersion of active metal became an outstanding problem for nanoparticles supported on inorganic matrix [23]. Catalytic hydrogenation of nitro aromatic compounds is one of the most important application of Pd based catalysts, due to their high activity under mild conditions compare to catalysts containing Ni, Fe or Pt active species [10, 24]. Catalytic hydrogenation of p-nitroaniline can be considered as an important reaction in the group of nitroaromatic catalytic hydrogenation reactions. Hydrogenation of p-nitroaniline is commonly used for synthesis of p- phenylenediamine an intermediate for aramid polymers production including Kevlar^{TM}, Twaron^{TM} [25, 26]. Typically reaction mechanism of p-nitroaniline hydrogenation contains several intermediates (Scheme 1) therefor reaction selectivity strongly depends on catalyst structure and operation conditions [5, 6, 8, 24].

Additionally in case providing catalytic hydrogenation of p-nitrobenzene in reactive solvents, especially in alcohols additional side reactions can take place under high pressure and temperature in case of catalyst low selectivity. Here the synthesis of Pd based nanoparticulate catalysts over alumina, silica, activated carbon providing high active metal dispersion is reported. Synthesized catalysts samples were characterized by different physicochemical methods including scanning electron microscopy, temperature programmed reduction, nitrogen physisorption, infrared spectroscopy and tested in p-nitroaniline catalytic hydrogenation process. Correlation of catalyst structure and its activity in p-nitro aniline hydrogenation process was found.

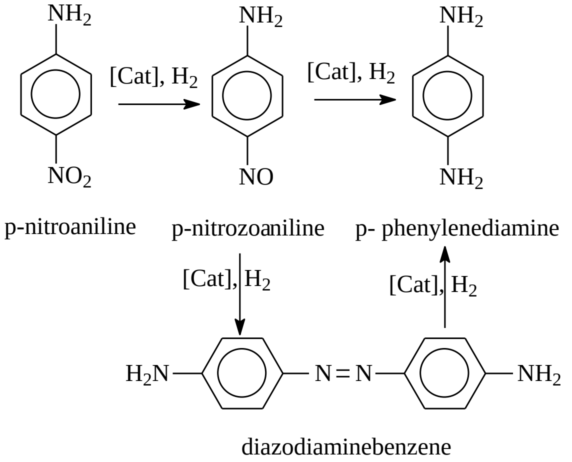

Scheme 1. Reaction scheme of p-nitroaniline catalytic hydrogenation
Схема 1. Реакционная схема каталитического гидрирования п-нитроанилина

EXPERIMENTAL

Chemicals and materials

Palladium chloride ($PdCl_2 \cdot 2H_2O$) (Vecton, Russia), sodium carbonate (Vecton, Russia), 2-propanol (99% Vecton, Russia). For the catalyst preparation high-purity gases (Ar 99.998%; H_2 99.999%) were used. Chemical grade Al_2O_3, activated carbon ARD-2 were purchased from Reachim Ltd. Russia and were used for catalyst synthesis as received.

Synthesis of silica

To synthesize spherical silica nanoparticles 700 ml of distilled water was added to 500 ml of 2-propanol in a flat-bottomed flask and solution was stirred for obtaining uniform solution. Then 200 ml of tetraethoxysilane was added to solution. The whole system was kept on mechanical stirrer for 30 min with mixing rate1500 rpm. Subsequently, the 50 ml of aqueous ammonia solution (60 wt. %) was added drop-wise to the reaction mixture during 30 min. The mixture was retained to stand for 120 min under stirring rate 1000 rpm. Then, the precipitate was filtered, washed with distilled water and dried at 473 K for 3 h on air.

Catalyst synthesis

Synthesis of Pd based catalysts was made by precipitation of palladium hydroxide due to hydrolysis reaction by addition of 3 mM H_2PdCl_4 solution in water to a 1g of support (SiO_2, γ-Al_2O_3, or activated carbon) suspended in 40 ml aqueous solution of 0.1 M Na_2CO_3 and 0.1M solution of sodium dodecyl sulfate using ultrasonic bath (Bandelin, 10P, Germany). The solution of H_2PdCl_4 was prepared in 0.1M hydrochloric acid (HCl). The suspension was mixed for 3 h at 308 K in ultrasonic bath. The catalysts sample was filtered, thoroughly washed with distilled water and dried at 338 K under air. Prior to kinetic experiments catalysts sample was reduced at 523 K for 60 min in the hydrogen flow in tube furnace than cooled to ambient temperature and flashed with nitrogen and immediately transferred to the catalytic reactor. Following samples were synthesized and denoted as 5 wt. % Pd/γ-Al_2O_3, 4 wt. % Pd/γ-Al_2O_3, 3 wt. % Pd/γ-Al_2O_3, 5 wt. % Pd/SiO_2, 4 wt. % Pd/SiO_2, 3 wt. % Pd/SiO_2, 5 wt. % Pd/C, 4 wt. % Pd/C, 3 wt. % Pd/C using this methodology.

Temperature programmed reduction (TPR) study of catalysts

Temperature-programmed reduction (TPR) experiments were performed at a heating rate of 5 K/min from 25 K to 573 K in a gas mixture consisting of 10% H_2 in Ar. Prior to reduction sample was flashed with helium for one hour at 378 K. Calibration was done by reduction of Ag_2O powder. The gas flow rate was maintained at 30 ml(STP)/min for all experiments. The TPR curves were obtained using automatic chemisorption analyzer AutoChem HP 2950 (Micromeritics, USA).

Scanning electron microscopy (SEM)

The morphological characteristics of catalysts samples were examined by scanning electron microscopy (SEM, TESCAN, Vega-LSU) equipped with X-ray microanalysis (OXFORD INCA PentaFETx3). Scanning electron microscope images were collected at a magnification of 66.1 kX at 20 kV with scaning electrone detector.

Nitrogen physisorption

Nitrogen adsorption-desorption isotherms were obtained at the normal boiling point of liquid nitrogen using a Beckman Coulter SA 3100 apparatus (Coulter Corporation, USA). Studied materials were preliminary degassed in a Beckman Coulter SA-PREP apparatus for sample preparation at 423 K in flow of inertial nitrogen.

Supports and catalysts study by Fourier transformation infrared spectroscopy (FTIR)

Qualitative and quantitative composition of studied materials surface was performed by diffuse reflectance IR spectroscopy using the IR-Fourier spectrometer IRPrestige-21 (Shimadzu, Japan) equipped with a diffuse reflection attachment DRS-8000 (Simadzu, Japan). All spectra were obtained in the wave number range 250-4000 cm^{-1} with a resolution of 4 cm^{-1}.

Pulse hydrogen chemisorption

Pulse chemisorption analysis was carried out in order to determine chemically-active metal's surface area and cumulative quantity of active metal by applying a pulse titration of the sample with the hydrogen. The patterns were obtained by means of AutoChem HP 2950 automatic chemisorption analyzer (Micromeritics, USA).

Catalysts activity experiments description

The activity of catalysts samples (5 wt. % Pd/γ-Al_2O_3, 4 wt. % Pd/γ-Al_2O_3, 3 wt. % Pd/γ-Al_2O_3, 5 wt. % Pd/SiO_2, 4 wt. % Pd/SiO_2, 3 wt. % Pd/SiO_2, 5 wt. % Pd/C, 4 wt. % Pd/C, 3 wt. % Pd/C) was studied in hydrogenation of p-nitroaniline to 1,4-phenylenediamine in water solution of 2-propanol (0.68 mole fraction). The process was performed in titanium reactor (300 ml) equipped with two-blade stirrer and temperature-control. The catalytic activity was evaluated by measuring hydrogen consumption rate using volumetric method and gas chromatography [27, 28]. A hydrogen consumption rates were calculated as inclination angle tangent of hydrogen consumption kinetic curves. The Sheldon's filtration test was performed to insure absence of homogeneous catalysis due to palladium leaching from the catalyst surface [29, 30]. After reaction finishing reactor was flashed with nitrogen, then catalyst was filtered and washed with water solution of 2-propanol and dried in vacuum drier for one hour for further physicochemical analysis.

RESULT AND DISCUSSION

The temperature-programmed reduction study of catalysts

Temperature-programmed reduction (TPR) profiles were obtained for 5 wt. % and 3 wt. % of catalysts to clarify particularities of palladium oxide and hydroxide reduction during catalysts activation in a stream of hydrogen. The TPR profiles collected for 5 wt. % Pd catalysts supported on silica, alumina and activated carbon are shown in figure 1. The deconvolution of resulting broad peaks represents a view about quantity and forms of Pd species during palladium transformation into metallic state (Fig. 1).

The physical meaning of a long plateau may be corresponded to reduction kinetics of different forms of palladium oxide and hydroxide to metallic palladium [31]. This process may be in a steady state for some time until the recovery of these forms of metal does not completely pass. According to the literature data, this absorption of hydrogen is associated with the reduction of palladium hydroxide and oxide films [31]. The absence of negative peaks also suggests that the path of the palladium species reduction does not include the stage of palladium hydrides decomposition [32-34]. Thus, it can be assumed that palladium oxide and palladium hydroxide reduces in to metallic palladium during catalysts treatment with hydrogen. The reduction process involves 4-6 reactions. According to the obtained profiles, it can be concluded that sufficient activation temperature should be higher than 373 - 393 K [35, 36].

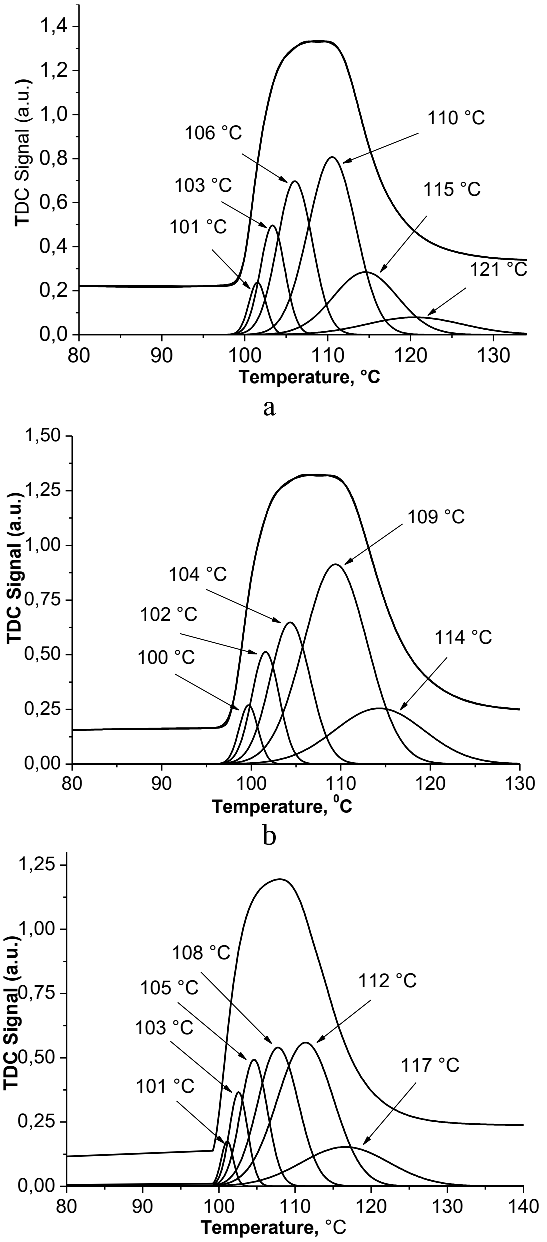

a

b

c

Fig. 1. The decomposition of TPR profile of a) 5 wt.% Pd/γ-Al_2O_3; 1-101 °C, 2-103 °C, 3-106 °C, 4- 110 °C, 5-115 °C, 6-121 °C b) 5 wt. % Pd/SiO_2; 1-100 °C, 2-102 °C, 3-104 °C, 4- 109 °C, 5-114 °C c) 5 wt. % Pd/C; 1-101 °C, 2-103 °C, 3-105 °C, 4- 108 °C, 5-112 °C, 6-117 °C
Рис. 1. Разложение профиля TPR a) 5 масс.% Pd/γ-Al_2O_3; 1-101 °C, 2-103 °C, 3-106 °C, 4- 110 °C, 5-115 °C, 6-121 °C b) 5 масс. % Pd/SiO_2; 1-100 °C, 2-102 °C, 3-104 °C, 4- 109 °C, 5-114 °C c) 5 масс. % Pd/C; 1-101 °C, 2-103 °C, 3-105 °C, 4- 108 °C, 5-112 °C, 6-117 °C

Scanning electron microscopy (SEM)

The SEM images (Fig. 2) show catalists particles befor activation, after activaton and after reaction. The surface of Pd catalist supported on alumina after reaction became more defect. The surface of silica based catalists remains stable during hydrogenation treatement and reaction.

Before activation After activation Catalyst samples after reaction

5% Pd/γ-Al_2O_3

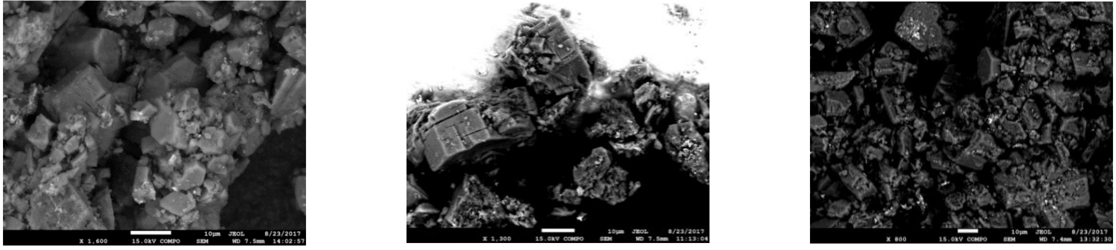

5% Pd/SiO_2

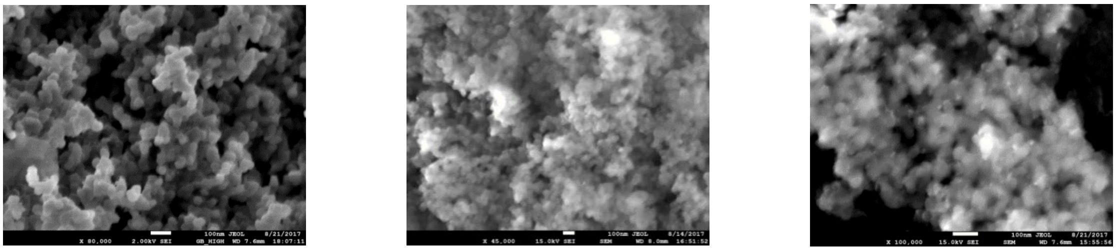

5% Pd/C

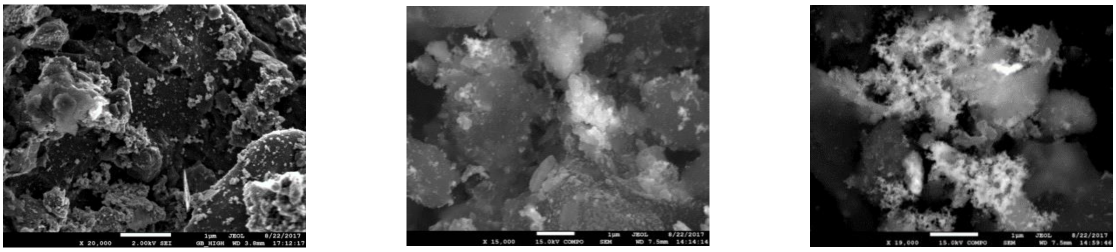

Fig. 2. The SEM images of catalysts
Рис. 2. SEM-изображения катализаторов

The average size of silica particles is 50-60 nm. The silica nanospheres presents as aggregated in all samples. The surface of acivated carbon change after activation due to palladium reduction and became more X-ray contrast. After p-nitrobenzene hydrogenation carbon based catalists shows some agregation of surface.

Nitrogen physisorption

The structural characteristics of the initial catalysts and after conducting 5 reaction cycles of 4-nitroaniline to 1,4-phenylenediamine hydrogenation are presented in table 1 and 2, the distributions of pore volumes are showed in tables 1s, 2s of supplementary materials.

According to the t-plot model, the presence of an internal surface was observed only for catalysts on activated carbon. But micro, meso and macropores presents on the surface of all samples. Due to the fact that the alumina morphology is crystalline, the absence of the internal pores and channels is the expected result. And it is quite clear that the external surface of alumina at the same time can have various defects and cracks. The absence of the inner surface for silica is an interesting detail, because usually the amorphous silica synthesized by the sol-gel method is characterized by the presence of a porous structure [37, 38].

Perhaps the catalytic phase of palladium formed on the inner surface in the pores. This explains the lack of internal surface in catalysts based on silica. The specific surface area according to Langmuir and BET for 5 wt. %, 4 wt. % Pd/SiO_2 catalysts after reaction increased by 1.5 times while for 3 wt. % Pd/SiO_2 sample specific surface area practically did not change. Increasing of surface area after reaction can be the result of the particles abrasion, as well as the leaching of soluble components remaining after synthesis in case of insufficient washing of the synthesized catalysts. The specific area of catalysts synthesized on γ-Al_2O_3 practically didn’t changes. And in the case of palladium catalysts synthesized on activated carbon, the specific surface area decreased 1.5 - 2 times, probably, due to activation carbon particles abrasion.

Table 1

The values of specific surface area of catalysts 1) - specific surface area of mesopores; 2) - specific surface area of micropores; 3) - specific surface area of macropores

***Таблица 1.* Значения удельной поверхности катализаторов 1) - удельная поверхность мезопор; 2)- удельная поверхность микропор; 3) - удельная поверхность макропор**

Catalyst	Specific surface area			
	The Langmuir adsorption model	The BET adsorption model	t-plot adsorption model	
	S_L, m^2/g	S_{BET}, m^2/g	$S_{external}$, m^2/g	$S_{internal}$, m^2/g
5 wt. % Pd/γ-Al_2O_3	95	103	$112^{1)}$ $130^{2)}$ $158^{3)}$	-
4 wt. % Pd/γ-Al_2O_3	97	105	$112^{1)}$ $127^{2)}$ $147^{3)}$	-
3 wt. % Pd/γ-Al_2O_3	104	111	$117^{1)}$ $134^{2)}$ $166^{3)}$	-
5 wt. % Pd/SiO_2	36	39	$45^{1)}$ $58^{2)}$ $68^{3)}$	-
4 wt. % Pd/SiO_2	31	36	$49^{1)}$ $68^{2)}$ $83^{3)}$	-
3 wt. % Pd/SiO_2	32	36	$49^{1)}$ $71^{2)}$ $88^{3)}$	-
5 wt. % Pd/C	759	727	$418^{1)}$ $250^{2)}$ $147^{3)}$	$309^{1)}$ $477^{2)}$ $580^{3)}$
4 wt. % Pd/C	777	745	$422^{1)}$ $258^{2)}$ $142^{3)}$	$323^{1)}$ $488^{2)}$ $603^{3)}$
3 wt. % Pd/C	712	679	$379^{1)}$ $249^{2)}$ $142^{3)}$	$313^{1)}$ $443^{2)}$ $550^{3)}$

FTIR of supports and catalysts

The FTIR spectra of initial catalysts samples, samples after activation with hydrogen and catalysts after 4-nitroaniline hydrogenation are presented on figures 2-4s. According to [39, 40] the large band between 1000 and 400 cm^{-1} can be attributed to characteristic absorption band of alumina and correspond to the stretching vibration of the Al-O-Al bond. Presence of carbon oxide and bicarbonate ions on catalysts surface is confirmed by two peaks between 1500 and 1370 cm^{-1}. These bands are still observed after the reduction of palladium by hydrogen, which indicates strong adsorption of these ions on the catalysts surface (3). However, the FTIR spectra of the spent catalysts have very weak bands at 1520 and 1386 cm^{-1} (4). The wide band at 2100 cm^{-1} for Pd/γ-Al_2O_3 and γ-Al_2O_3 samples confirmed the presence of water. This band disappeared after catalyst treatment in a stream of hydrogen at 573 K (3). Superposition of hydroxyl groups vibration bands and tensile vibrations of adsorbed water molecules led to formation of a very large band centered near 3470 cm^{-1} [40].

Table 2

The values of specific surface area of catalysts after reaction 1) - specific surface area of mesopores; 2) - specific surface area of micropores; 3) - specific surface area of macropores

***Таблица 2.* Значения удельной поверхности катализаторов после реакции 1) - удельная поверхность мезопор; 2) - удельная поверхность микропор; 3) - удельная поверхность макропор**

Catalyst	Specific surface area			
	The Langmuir adsorption model	The BET adsorption model	t-plot adsorption model	
	S_L, m^2/g	S_{BET}, m^2/g	$S_{external}$, m^2/g	$S_{internal}$, m^2/g
5 wt. % Pd/γ-Al_2O_3	96	100	$106^{1)}$ $119^{2)}$ $139^{3)}$	-
4 wt. % Pd/γ-Al_2O_3	96	103	$110^{1)}$ $125^{2)}$ $151^{3)}$	-
3 wt. % Pd/γ-Al_2O_3	96	101	$109^{1)}$ $122^{2)}$ $146^{3)}$	-
5 wt. % Pd/SiO_2	55	57	$60^{1)}$ $67^{2)}$ $72^{3)}$	-
4 wt. % Pd/SiO_2	48	50	$52^{1)}$ $60^{2)}$ $66^{3)}$	-
3 wt. % Pd/SiO_2	53	55	$58^{1)}$ $67^{2)}$ $75^{3)}$	-
5 wt. % Pd/C	598	593	$359^{1)}$ $235^{2)}$ $120^{3)}$	$234^{1)}$ $357^{2)}$ $472^{3)}$
4 wt. % Pd/C	592	582	$363^{1)}$ $220^{2)}$ $121^{3)}$	$217^{1)}$ $360^{2)}$ $459^{3)}$
3 wt. % Pd/C	478	474	$312^{1)}$ $191^{2)}$ $123^{3)}$	$160^{1)}$ $279^{2)}$ $350^{3)}$

In case of catalysts synthesized on silica the vibrations of hydrogen bond molecules (OH) appeared as bands centered at 3420-3468 cm^{-1}. The stretching and deformation vibrations of adsorbed water molecules give a signal at wavelength about 1640 cm^{-1}. The

PdO/SiO_2 spectra has large peak centered around 2941 cm^{-1}, which is associated to the deformation of the C-H group: >CH-, $-CH_2-$ and $-CH_3$ (2). It means the hydrolysis of tetraethoxysilane was incomplete carried out. As result the surface methyl silica was formation. This was certified by broad peak in the range 1338-1500 cm^{-1} that can be assigned to the C-H deformation vibrations of aliphatic bands [41]. The intense bands appearing at 1059-1176 cm^{-1} can be attributed to asymmetric Si-O-Si stretching vibrations [41]. The spectra of Pd on gamma-alumina and silica are comparable. In the case of activated carbon and catalysts synthesized on activated carbon the vibrations of carboxyl and hydroxyl groups and other oxygen-containing surface groups appeared in the range from 500 to 2000 cm^{-1} [42]. The deformation vibrations of the C=O group can be attributed to the peaks in the range of 1635-1600 cm^{-1} and the formation vibrations of C-O-R group to the peak at 1014 cm^{-1} [42].

The deformational-symmetric and asymmetric vibrations of the C-O group can be corresponded to the weak peaks at 2360 cm^{-1}, 1030 cm^{-1} [42, 43]. The sample of palladium on activated carbon 3 wt. % Pd/C has some difference in spectrum. For this sample a broad deformation vibrations lines of O-C=O, O-C-O presence in range 752-800 cm^{-1} [43]. The bands in the range of 1217–1085 cm^{-1} can be associated with the region of C-C skeletal vibrations (4) [43].

The pulse chemisorption study

The Pd catalysts synthesized on silica are characterized by largest specific surface area of active metals (0.8-1.3 m^2/g), while Pd catalysts synthesized on alumina and carbon have lower specific surface of active metal (0.6-0.7 m^2/g).

Table 3

Catalysts surface characteristics

***Таблица* 3. Характеристики поверхности катализаторов**

catalyst	$Pd/\gamma\text{-}Al_2O_3$			Pd/SiO_2			Pd/C		
Content of Pd, wt. %	5%	4%	3%	5%	4%	3%	5%	4%	3%
S_{metal}, m^2/g_{sample}	0.7	0.7	0.7	1.1	0.8	1.3	0.7	0.6	0.7
Cumulative quantity, mmol/g	15	14	14	24	16	28	13	12	14
Chemisphere size, nm	34.6	29.5	22.2	21.7	26.4	11.3	39.1	35.0	22.3

This result can be attributed to stronger interaction of silica surface with palladium nanoparticle, preventing it from aggregation.

The activity of synthesized catalysts

According to the UV-VIS spectroscopy data in all cases the hydrogenation of p-nitroaniline to p-phenylenediamine was close to 100% conversion. The examples of absorption spectra are shown in Fig. 6s. The kinetic curves of hydrogen consumption are shown in Fig. 6-8s. Comparison of initial activity of synthesized samples (Fig. 3) shows strong correlation of specific hydrogen consumption rate on mean diameter of palladium nanoparticles in catalysts. The increase of hydrogen consumption with decrease of average palladium nanoparticles diameter can be attributed to better accessibility of small nanoparticles to hydrogen and substrate that correlate to literature data [44, 45].

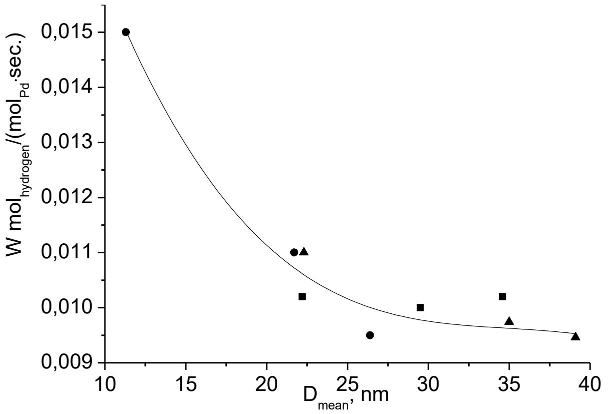

Fig. 3. Comparison of developed catalysts specific catalytic activity on mean diameter of nanoparticles. ● – Pd/SiO_2; ▲ – Pd/C; ■ – $Pd/\gamma\text{-}Al_2O_3$

Рис. 3. Сравнение удельной каталитической активности разработанных катализаторов по среднему диаметру наночастиц. ● – Pd/SiO_2; ▲ – Pd/C; ■ – $Pd/\gamma\text{-}Al_2O_3$

Catalytic activity of 5 wt. %, 4 wt. % and 3 wt. % $Pd/\gamma\text{-}Al_2O_3$ samples in 5 repeated cycles decreased by ~29.3%, ~32.6% and ~33.3% compare to initial activity. Evaluation catalytic activity changes of palladium catalysts synthesized on activated carbon showed hydrogenation rate decrease for 27% - 34% after the 5 reaction cycle. Catalytic activity of palladium catalysts synthesized on silica showed hydrogenation rate decrease for 10-30% after the 5 reaction cycle. Visible decrease of catalytic activity in repeated cycles can be attributed to product adsorption over active sites of palladium species.

Conclusion

A series of palladium based catalysts were synthesized using alumina, silica and activated carbon as nanoparticles supports and characterized by different physicochemical methods. Formation of metal palladium nanoparticles with mean diameter 10-40 nm on the support surface was observed during synthesis and palladium reduction by hydrogen. Different forms of palladium oxide and hydroxide were observed during reduction of active metal species in initial catalysts to metallic palladium. FTIR spectra of synthesized catalysts show palladium interaction with catalysts matrix.

Strong correlation of catalysts nanoparticles mean diameter with hydrogen consumption specific activity was noticed. The increase of active metal nanoparticles diameter from 10 nm to 20 nm results in appropriate decrease of hydrogen specific consumption from 0.015 $mol(H_2)/(mol(Pd)\cdot s)$ down to 0.010 $mol(H_2)/(mol(Pd)\cdot s)$. Further increase of active metal nanoparticle diameter does not affect catalysts activity. The increase of hydrogen consumption rate with decrease of average palladium nanoparticles diameter can be attributed to better accessibility of small nanoparticles to hydrogen and substrate.

Acknowledgments

This work is funded by the Russian Science Foundation under grant №18-79-10157.

REFERENCES
ЛИТЕРАТУРА

1. **Nicolaou K.C.** Catalyst: Synthetic Organic Chemistry as a Force for Good. *Chem*. 2016. V. 1. P. 331-338. DOI: 10.1016/j.chempr.2016.08.006.
2. **Baig R.B.N., Varma R.S.** Magnetically retrievable catalysts for organic synthesis. *Chem. Commun*. 2013. V. 49. P. 752-770. DOI: 10.1039/C2CC35663E.
3. **Climent M.J., Corma A., Iborra S.** Heterogeneous catalysts for the one-pot synthesis of chemicals and fine chemicals. *Chem. Rev.* 2011. V. 111. P. 1072-1133. DOI: 10.1021/cr1002084.
4. **Navneet Sharma, Himanshu Ojha, Ambika Bharadwaj, Dharam Pal Pathak, Rakesh Kumar Sharma.** Preparation and catalytic applications of nanomaterials: a review. *RSC Adv*. 2015. V. 5. N 66. P. 53381-53403. DOI: 10.1039/C5RA06778B.
5. **Santosh Bahadur Singh, Praveen Kumar Tandon**. Vapor phase hydrogenation of nitrobenzene to aniline over carbon supported ruthenium catalysts. *J. Nanosci. Nanotechnol.* 2015. V. 15. P. 5403-5409. DOI: 10.1166/jnn.2015.9872
6. **Zhao F., Ikushima Y., Arai M.** Hydrogenation of nitrobenzene with supported platinum catalysts in supercritical carbon dioxide: effects of pressure, solvent, and metal particle size. *J. Catal.* 2004. V. 224. P. 479-483. DOI: 10.1016/j.jcat.2004.01.003.
7. **Relvas J., Andrade R., Freire F.G., Lemos F., Araujo P., Pinho M.J., Nunes C.P., Ribeiro F.R.** Liquid phase hydrogenation of nitrobenzene over an industrial Ni/SiO_2 supported catalyst. *Catal. Today*. 2008. V. 133. P. 828-835. DOI: 10.1016/j.cattod.2007.11.050.
8. **Figueras F., Coq B.** Hydrogenation and hydrogenolysis of nitro-, nitroso-, azo-, azoxy- and other nitrogen-containing compounds on palladium. *J. Molec. Catal. A: Chem*. 2001. V. 173. N 1. P. 223-230. DOI: 10.1016/S1381-1169(01)00151-0.
9. **Yu X., Wang M., Li H.** Study on the nitrobenzene hydrogenation over a $Pd-B/SiO_2$ amorphous catalyst. *Appl. Catal. A: Gen*. 2000. V. 202. N 1. P. 17-22. DOI: 10.1016/S0926-860X(00)00454-3.
10. **Sudhakar D.M., lakshmi Kantam M., Ramineni K., Naveen Kumar S., Akula V.** Vapour phase hydrogenation of nitrobenzene over metal (Ru, Ni, Pt, Pd) supported on $Ca_5(PO_4)3(OH)$ catalysts. *J. Nanosci. Nanotechnol*. 2014. V. 53. N 7. P. 5403–5409. DOI: 10.1166/jnn.2015.9872.
11. **Rogers S.M., Catlow C.R.A., Chan-Thaw C.E., Chutia A., Jian N., Palmer R.E., Perdjon M., Thetford A., Dimitratos N., Villa A., Wells P.P.** Tandem site- and size-controlled pd nanoparticles for the directed hydrogenation of furfural. *ACS Catal.* 2017. V. 7. N 4. P. 2266-2274. DOI: 10.1021/acscatal.6b03190.
12. **Sher shah M. S. A., Guin D., Sunkara M.** Pd @ PEG-PU polymer networks: a convenient catalyst for hydrogenation and Suzuki coupling reactions. *Mater. Chem. Phys*. 2010. V. 124. N 1. P. 664-669. DOI: 10.1016/j.matchemphys.2010.07.031.
13. **Makowski W., Sobczak J., Król A.** Acetophenone hydrogenation on polymer–palladium catalysts. The effect of polymer matrix. *Catal. Lett.* 2004. V. 94. N 3–4. P. 143-156. DOI: 10.1023/B:CATL.0000020539.31128.d4.
14. **Králik M., Vallušová Z., Major P., Takáčová A., Hronec M., Gašparovičová D.** Hydrogenation of chloronitrobenzenes over Pd and Pt catalysts supported on cationic resins. *Chem. Papers*. 2014. V. 68. P. 1690-1700. DOI: 10.2478/s11696-014-0565-3.
15. **Dai C., Liu F., Zhang W., Li Y., Ning C., Wang X., Zhang C.** Deactivation study of Pd/Al_2O_3 catalyst for hydrogenation of benzonitrile in fixed-bed reactor. *Appl. Catal. A: Gen*. 2017. V. 538. P. 199-206. DOI: 10.1016/j.apcata.2017.03.030.
16. **Komhom S., Mekasuwandumrong O., Praserthdam P., Panpranot J.** Improvement of Pd/Al_2O_3 catalyst performance in selective acetylene hydrogenation using mixed phases Al_2O_3 support. *Catal. Commun*. 2008. V. 10. N 1. P. 86-91. DOI: 10.1016/j.catcom.2008.07.039.
17. **Boudjahem A.-G., Redjel A., Mokrane T.** Preparation, characterization and performance of Pd/SiO_2 catalyst for benzene catalytic hydrogenation. *J. Indust. Eng. Chem.* 2012. V. 18. N 1. P. 303-308. DOI: 10.1016/j.jiec.2011.11.038.
18. **Horváth A., Beck A, Koppány Z., Sárkány A., Guczi L.** Sol-derived Pd/SiO_2 catalyst: characterization and activity in benzene hydrogenation. *J. Molec. Catal. A: Chem*. 2002. V. 182-183. P. 295-302. DOI: 10.1016/S1381-1169(01)00480-0.
19. **Song X., Wu Y., Pan D., Zhang J., Xu S., Gao L, Wei R., Xiao G.** Functionalized DVB-based polymer catalysts for glycerol and CO_2 catalytic conversion. *J. CO_2 Utilization*. 2018. V. 28. P. 326-334. DOI: 10.1016/j.jcou.2018.10.015.
20. **Luo Y., Xie W., Huang Y., Zhang T., Yang B., Liu Y., Zhou X., Zhang J.** Polydimethylsiloxane sponge supported DMAP on polymer brushes: Highly efficient recyclable base catalyst and ligand in water. *J. Catal.* 2018. V. 367. P. 264. DOI: 10.1016/j.jcat.2018.09.015.
21. **Tungler A., Szabados E.** Overcoming problems at elaboration and scale-up of liquid-phase pd/c mediated catalytic hydrogenations in pharmaceutical production. *Org. Proc. Res. Develop*. 2016. V. 20. N 7. P. 1246-1251. DOI: 10.1021/acs.oprd.6b00073.
22. **Wichner N.M., Beckers J., Rothenberg G., Koller H.** Preventing sintering of Au and Ag nanoparticles in silica-based hybrid gels using phenyl spacer groups. *J. Mater. Chem*. 2010. V. 20. P. 3840-3847. DOI: 10.1039/C000105H.
23. **Rudolf C., Mazilu I., Chirieac A., Dragoi B., Abi-Ghaida F. Ungureanu A., Mehdi A., Dumitriu E.** Copper nanoparticles supported on polyether-functionalized mesoporous silica. synthesis and application as hydrogenation catalysts. Environ. Eng. Manag. J. 2015. V. 14. P. 399-408. DOI: 10.30638/eemj.2015.041.
24. **Tong S.B., O'Driscoll K.F., Rempel G.L.** Kinetics of nitrobenzene hydrogenation using a gel entrapped palladium catalyst. *Canad. J. Chem. Eng.* 1978. V. 56. P. 340-345. DOI: 10.1002/cjce.5450560311.
25. **Okajima I., Okamoto H., Sako T.** Recycling fiber-reinforced plastic using supercritical acetone. *Polym. Degrad. Stabil.* 2019. V. 163. P. 1-6. DOI: 10.1016/j.polymdegradstab.2019.02.018.

26. **Vemu Vara Prasad, Sowjanya Talupula.** A review on reinforcement of basalt and aramid (Kevlar 129) fibers. *Mater. Today: proceed.* 2018. V. 5. N 2. P. 5993-5998. DOI: 10.1016/j.matpr.2017.12.202.
27. **Coq B., Figueras F.** Structure - activity relationships in catalysis by metals: some aspects of particle size, bimetallic and supports effects. *Coord. Chem. Rev.* 1998. V. 178. P. 1753-1783. DOI: 10.1016/S0010-8545(98)00058-7.
28. **McMillan L., Gilpin L.F., Baker J., Brennan C., Hall A., Lundie D.T., Lennon D.** The application of supported palladium catalysts for the hydrogenation of aromatic nitriles. *J. Molec. Catal. A: Chem.* 2016. V. 411. P. 239-246. DOI: 10.1016/j.molcata.2015.10.028.
29. **Lempers H.E.B., Sheldon R.A.** The stability of chromium in CrAPO-5, CrAPO-11, and CrS-1 during liquid phase oxidations. *J. Catal.* 1998. V. 175. P. 62-69. DOI: 10.1006/jcat.1998.1979.
30. **Lazar A., Silpa S., Vinod C.P., Singh A.P.** A heterogeneous route for transfer hydrogenation reactions of ketones using Ru(II)Cymene complex over modified benzene-organosilica (PMOB). *Molec. Catal.* 2017. V. 440. P. 66-74. DOI: 10.1016/j.mcat.2017.07.018.
31. **Ivanova A., Slavinskaya E., Gulyaev R., Zaikovskii V., Stonkus O., Danilova I., Plyasova L., Polukhina I., Boronin A.** Metal–support interactions in Pt/Al_2O_3 and Pd/Al_2O_3 catalysts for CO oxidation. *Appl. Catal. B: Environ.* 2010. V. 97. P. 57-71. DOI: 10.1016/j.apcatb.2010.03.024.
32. **Zheng Q., Farrauto R., Deeba M.** Part II: Oxidative thermal aging of Pd/Al_2O_3 and Pd/Ce_xO_y-ZrO_2 in automotive three way catalysts: the effects of fuel shutoff and attempted fuel rich regeneration. *Catalysts.* 2015. V. 5. P. 1797-1814. DOI: 10.3390/catal5041797.
33. **Nag N.K.** A Study on the formation of palladium hydride in a carbon-supported palladium catalyst. *J. Phys. Chem. B.* 2001. V. 105. P. 5945-5949. DOI: 10.1021/jp004535q.
34. **Gil S., Liotta L., Pantaleo G., Ousmane M., Retailleau-Mevel L., Giroir-Fendler A.** Catalytic oxidation of propene over Pd catalysts supported on CeO_2, TiO_2, Al_2O_3 and M/Al_2O_3 oxides (M=Ce, Ti, Fe, Mn). *Catalysts.* 2015. V. 5. P. 671-689. DOI: 10.3390/catal5020671.
35. **Zhu H., Qin Z., Shan W., Shen W., Wang J.** Pd/CeO_2–TiO_2 catalyst for CO oxidation at low temperature: a TPR study with H_2 and CO as reducing agents. *J. Catal.* 2004. V. 225. P. 267-277. DOI: 10.1016/j.jcat.2004.04.006 (2004).
36. **Thompson S.T.** Palladium-rhenium catalysts for selective hydrogenation of furfural: evidence for an optimum surface composition. *ACS Catal.* 2016. V. 6. N 11. P. 7438–7447. DOI: 10.1021/acscatal.6b01398.
37. **Kumar S., Malik M.M., Purohit R.** Influence of tool revolving on mechanical properties of friction stir welded 5083aluminum alloy. *Mater. Today: Proceed.* 2017. V. 4. P. 350-335. DOI: 10.1016/j.matpr.2017.01.029.
38. **Han W., Jia Y., Yao N., Yang W, He M., Xiong G.** A novel template-free sol–gel synthesis of silica materials with mesoporous structures and zeolitic walls. *J. Sol-Gel Sci. Technol.* 2007. V. 43. P. 205-211. DOI: 10.1007/s10971-007-1564-4.
39. **Saikia B., Parthasarathy G.** Fourier transform infrared spectroscopic characterization of kaolinite from assam and meghalaya, Northeastern India. *J. Mod. Phys.* 2010. V. 1. P. 206-210. DOI: 10.4236/jmp.2010.14031.
40. **Jafar Tafreshi M., Masoomi Z.** Infrared spectroscopy studies on sol-gel prepared alumina powders. *Mater. Sci. (Medžiagotyra).* 2015. V. 21. N 1. P. 1392–1320. DOI: 10.5755/j01.ms.21.1.4872.
41. **Chukin G.D., Malevich V.I.** Infrared spectra of silica. *J. Appl. Spectrosc.* 1977. V. 26. N 2. P. 223-229. DOI: 10.1007/BF00615613.
42. **Cao J., Xiao G., Xu X., Shen D., Jin B.** Study on carbonization of lignin by TG-FTIR and high-temperature carbonization reactor. *Fuel Proc. Technol.* 2013. V. 106. P. 41-47. DOI: 10.1016/j.fuproc.2012.06.016.
43. **He X., Liu X., Nie B., Song D.** FTIR and Raman spectroscopy characterization of functional groups in various rank coals. *Fuel.* 2017. V. 206. P. 555-563. DOI: 10.1016/j.fuel.2017.05.101.
44. **Ganiyu S.A., Alhooshani K., Ali S.A.** Single-pot synthesis of Ti-SBA-15-NiMo hydrodesulfurization catalysts: Role of calcination temperature on dispersion and activity. *Appl. Catal. B: Environ.* 2017. V. 203. P. 428-441. DOI: 10.1016/j.apcatb.2016.10.052.
45. **Ortega-Dominguez R.A., Vargas-Villagran H., Penaloza-Orta C., Saavedra-Rubio K., Bokhimi X., Klimova T.E.** A facile method to increase metal dispersion and hydrogenation activity of Ni/SBA-15 catalysts. *Fuel.* 2017. V. 198. P. 110-122. DOI: 10.1016/j.fuel.2016.12.037.

Поступила в редакцию 16.01.2019
Принята к опубликованию 18.04.2019

Received 16.01.2019
Accepted 18.04.2019